Journal of Materials Chemistry C

Accepted Manuscript

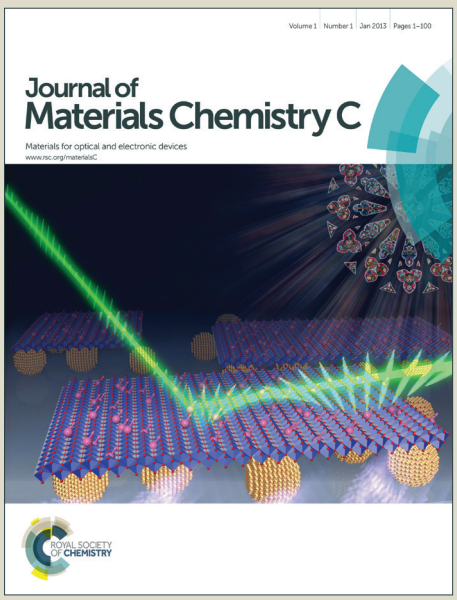

ROYAL SOCIETY OF CHEMISTRY

www.rsc.org/materialsC

Journal Name

RSCPublishing

ARTICLE

Amino-decorated lanthanide (III) – organic extended frameworks for multi-color luminescence and fluorescence sensing

Cite this: DOI: 10.1039/x0xx00000x

Received 00th January 2012,
Accepted 00th January 2012

DOI: 10.1039/x0xx00000x

www.rsc.org/

Ji-Na Hao, Bing Yan*

Solvothermal reactions of $LnCl_3 \cdot 6H_2O$ (Ln = Eu, Tb, Sm and Dy) with 2-aminoterephthalic acid obtain four isostructural lanthanide (III) – organic frameworks. The structure has the topology of a gadolinium 2-aminoterephthalic acid (MOF-LIC-1). The as-obtained samples were characterized by X-ray diffraction, FT-IR, TGA and luminescence spectroscopy. They all belong to the luminescence materials system with broad excitation band, whose excitation bands could extend to the visible light region. The selected ligand could effectively sensitize the luminescence of Eu^{3+}, Tb^{3+} and Sm^{3+}, especially the Eu^{3+} ions, thus leading to the characteristic luminescence of Ln^{3+}. More significantly, the white light emission could be realized by a single component Sm(III) framework. Furthermore, Eu-MOF was selected as a representative sample to examine the potential of the material for the sensing of metal ions and it showed highly selective and sensitive luminescence sensing for Al^{3+} ions. And the luminescence color change can be easily distinguished with the naked eye under the UV light irradiation.

Introduction

As a new class of porous materials, metal-organic frameworks, a class of crystalline hybrid inorganic-organic materials formed by the connection of metal centers or clusters and organic linkers, have attracted tremendous attention for their wide applications in the areas of gas storage/separation[1,] catalysis[2], magnetism[3], drug delivery[4,] sensors and luminescent probes[5], etc. Among the applications, particular interest is the very recently developed MOF-based luminescent sensing of ions and small organic molecules. For this application, in light of the excellent luminescent merits of lanthanide such as extremely sharp emissions, high color purity, and relatively long luminescence lifetimes, among the fruitful production of functional MOFs reported to date, of particular note are those luminescent lanthanide MOFs (Ln-MOFs), which can be viewed as the most promising class of materials for luminescent sensors and probes for chemical species[6].

To obtain effective MOF sensor, the binding site and powerful luminophore are needed[7]. Therefore, it is important to select appropriate ligands. On one hand, when constructing Ln-MOFs, the organic ligands can not only serve as connective building blocks for the structure but also function as antennae for the lanthanide ions[8]. In view of previous work[9], carboxylate-based ligands are a good choice because the Ln^{3+} ions are hard acceptors, making coordination with the hard carboxylate oxygen atoms more favorable according to the "hard-soft acid-base" concept. What's more, aromatic carboxylic groups are good luminescent chromophores, resulting in the intense luminescence of lanthanide. On the other hand, fabricating Ln-MOFs possessing functional sites for specific luminescent selectivity recognition, however, has been still challenging. Alternatively, pyridyl nitrogen[6b,10] and amino nitrogen[11] can be considered as binding sites and be immobilized in luminescent MOFs. Since the "hard acid" of Ln^{3+} is not affinitive to the "soft base" N atom, when the ligand reacts with Ln^{3+}, the N atoms in the ligand are always uncoordinated[12]. Therefore, these preserved N sites acting could interact with other metal ions , leading to luminescence intensity changes of Ln^{3+} and further realizing the luminescent Ln-MOFs for sensing application. To summarize, considering the above two factors, an effective strategy to synthesize Ln-MOF sensors is to use π-conjugated organic molecules with Lewis basic site, in which π-conjugated organic molecules provide the powerful luminescence and rigid backbones and Lewis basic site provides the metal ion binding sites.

For this purpose, 2-amino-1,4-benzendicarboxylic acid (NH_2-BDC) was selected as the ligand to react with $LnCl_3 \cdot 6H_2O$ (Ln = Eu, Tb, Sm, Dy) under solvothermal conditions, generating a series of Ln-MOFs, isostructural to MOF-LIC-1(Gd)[13]. Herein, the syntheses, structure studies, luminescent properties and sensing properties of Ln-MOF-LIC-1 are examined and discussed. From the luminescent results, the selected ligand could effectively sensitize the luminescence of Eu^{3+}, Tb^{3+} and Sm^{3+}, especially the Eu^{3+} ions. It's worth noting that white light emission could be realized by the single component Sm(III) framework for its visible luminescence consists of blue ligand-centered emission (450 nm), green (563 nm), orange (598 nm) and red (645 nm) emission bands, which provides a promising single component approach to achieve white light emitting materials. Based on the luminescence study, the Eu-MOF was selected to explore the sensing behavior for metal ions and it

displays a sensing function with respect to Cu^{2+}, Fe^{2+}, Fe^{3+}, Al^{3+}, particularly Al^{3+}. Studies on the diffusion of Cu^{2+}, Fe^{2+}, Fe^{3+} and Al^{3+} have provided direct information of visibly luminescent color change with naked eyes under UV-light irradiation. For the Cu^{2+}, Fe^{2+} and Fe^{3+}, the luminescence is essentially completely quenched from the photographs. While for Al^{3+}, although it also completely quench the red-emitting of Eu^{3+} like the above three metal ions, the luminescence colors have changed to bright blue, thus we can easily recognize it. Therefore, Eu-MOF could be considered as luminescent probes toward certain metal ions - Al^{3+}. As we all know, Al^{3+} ions can be toxic to humans in excessive amounts. Many symptoms can all be caused by aluminum toxicity such as Alzheimer's disease and osteoporosis, rickets, anemia, softening of the bones, and so on. Due to the frequent use of aluminum cookware and cans, drinking water supplies, antacids, deodorants and bleached flour, the risk of absorption of Al^{3+} ions by the human body is increasing. Hence, selective detection or sensing of Al^{3+} seems to be important for human health.

Experimental section

Materials and instrumentation. The salts of $LnCl_3 \cdot 6H_2O$ were prepared by dissolving the corresponding lanthanide oxide compounds in excess hydrochloric acid (37 %) followed by evaporation and crystallization. 2-aminoterephthalic acid (99 %, NH_2-BDC) was purchased from Aldrich and used directly without further purification. All the other starting materials and reagents were all AR and used as purchased. The crystalline phases of the products were determined by X-ray powder diffraction patterns (XRD) using a Rigaku D/max-Rb diffractometer equipped with Cu anode, employing a scanning rate of 1 degree / min in the 2θ range of 8 – 20 °. Fourier transform infrared spectra (FTIR) were recorded with a Nexus 912 AO446 infrared spectrum radiometer within the wavenumber range 4000 – 400 cm^{-1} using the KBr pressed technique. Excitation and emission spectra of the solid samples were obtained on Edinburgh FLS920 spectrophotometer. Thermogravimetric analysis (TG) was measured using a Netzsch STA 449C system at a heating rate of 5 K min^{-1} under the nitrogen protection. Luminescence lifetime measurements were carried out on an Edinburgh FLS920 phosphorimeter using a 450 W xenon lamp as excitation source. The outer absolute luminescent quantum efficiency was determined using an integrating sphere (150 mm diameter, $BaSO_4$ coating) from an Edinburgh FLS920 phosphorimeter. The quantum yield can be defined as the integrated intensity of the luminescence signal divided by the integrated intensity of the absorption signal. The absorption intensity was calculated by subtracting the integrated intensity of the light source with the sample in the integrating sphere from the integrated intensity of the light source with a blank sample in the integrating sphere.

Synthetic procedures.

Synthesis of Ln-MOF (Ln = Eu, Tb, Sm, Dy)[13]

Ln-MOF were synthesized through a similar process from MOF-LIC-1(Gd) as follow: The ligand NH_2-BDC (361 mg, 2.00 mmol) were dissolved in DMF (20 mL) in a 100 mL Teflon-lined autoclave, and 1.33 mmol $LnCl_3 \cdot 6H_2O$ dissolved in DMF (10 mL) were then added to the mixture. After the contents were well mixed, the Teflon cell was sealed in the autoclave and heated in oven for 20 h at 120 °C. It resulted in a yellow single-crystal, which was filtered off, washed with DMF, and dried at room temperature under vacuum.

Luminescence sensing experiment[5d]

Eu-MOF powders (3 mg) were simply immersed in the DMF solutions of MCl_z (10^{-2} mol/L, 3mL) at room temperature ($M^{z+} = Li^+$, Cu^{2+}, Zn^{2+}, Cd^{2+}, Mn^{2+}, Fe^{3+}, Fe^{2+}, Ni^{2+}, Al^{3+}, respectively). Then, the mixtures were sonicated for five minutes to form the metal ion incorporated suspension for luminescent measurements.

Results and discussion

Characterization of Ln-MOF (Ln = Eu, Tb, Sm and Dy)

The four compounds were solvothermally synthesized from a mixture of $LnCl_3 \cdot 6H_2O$ (Ln = Eu, Tb, Sm, Dy), 2-aminoterephthalic acid (NH_2-BDC) and DMF. The PXRD pattern (Figure 1) of the four compounds is all in good agreement with the Gd-MOF, revealing that the framework topology of all the four compounds is isostructural with a gadolinium 2-aminoterephthalic acid (MOF-LIC-1)[13].

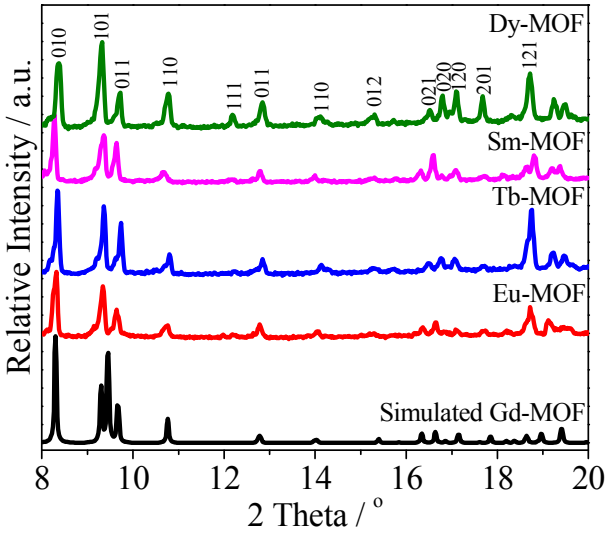

Figure 1 PXRD pattern of Ln-MOF.

The as-prepared Ln-MOF was also monitored by FTIR spectra and TG analysis. The IR spectra of the four compounds (Figure S1) are similar, further confirming their isostructure. The two absorption bands appearing at ~3460 and ~3342 cm^{-1} are assigned to the stretching vibrations of N-H, and the broad band at ~3500 originating from υ(OH) is not observed in the spectra, confirming the complete deprotonation of the NH_2-BDC ligand. The peaks at ~1662 and ~ 1504 cm^{-1} are attributed to the asymmetric and symmetric stretching vibrations of C=O, respectively. Compared with the free carboxyl groups whose absorption band of C=O is at ~1700 cm^{-1}, the lower wavenumber of υ(C=O) indicates the coordination between carboxyl groups and Ln^{3+}. The strongest band at ~ 1376 is produced by the amino C-N stretch[14]. The TGA diagram of the Eu-MOF (Figure S2) shows two main weight losses in the

curves. The first weight loss of 12.7% (cal. 11.8%) was in the temperature range of 200 – 300 °C, corresponding to the loss of coordinated DMF molecules. A further mass loss 34.7% occurs from 300 to 800 °C, ascribed to the decomposition of the framework and the release of the ligand composite (cal. 38.7%). The final residues are composed of Eu_2O_3.

Photoluminescent properties.

The luminescent properties of the four complexes and ligands in the solid state were investigated at room temperature. The excitation spectra (Figure 2, 3 and Figure S3, S6) indicates the compounds belong to the luminescence materials system with broad excitation band, whose excitation bands all extend to the visible light region. The luminescence spectrum on Eu-MOF is shown in Figure 2a. When excited at 333 nm, the compound exhibits the characteristic peaks at 579, 593, 614, 650 and 697 nm, which can be assigned to $^5D_0 \rightarrow {}^7F_J$ (J = 0 — 4) transitions of the Eu^{3+} ions, respectively. Under UV-light irradiation, Eu-MOF shows strong red luminescence which can be readily observed by naked eye, as shown in the inset of Figure 2a, indicating the antenna effect occurs. The emission spectrum of Tb-MOF in Figure 2b shows all the transitions from the emitting $^5D_4$ level to the ground-state manifold (487 nm, $^5D_4 \rightarrow {}^7F_6$; 545 nm, $^5D_4 \rightarrow {}^7F_5$; 580 nm, $^5D_4 \rightarrow {}^7F_4$; and 619 nm, $^5D_4 \rightarrow {}^7F_3$). The maximum of the emission at 545 nm contributes to the green-emitting color, as shown in the inset of Figure 2b.

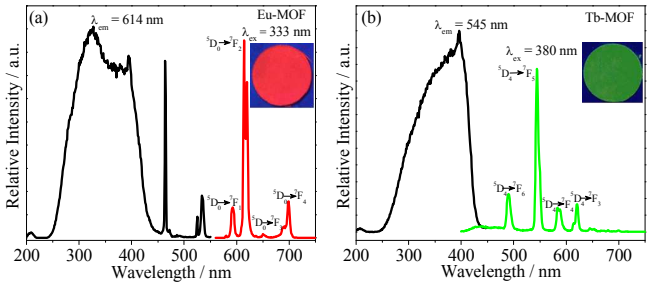

Figure 2 Excitation (black line) and emission spectra of Eu-MOF (a) and Tb-MOF (b). The insets are the corresponding luminescence pictures under UV-light irradiation of 365 nm.

For both Eu and Tb-MOF, the ligand-centered emission is not detected in their emission spectra, implying the existence of an efficient ligand-to-Ln(III) energy transfer process. While for Sm-MOF, the ligand-centered emission centered at 450 nm can be observed in Figure 3a. Compared to the emission band of the free ligand (570 nm for NH_2-BDC, Figure S3), the blue-shift of the ligand emission when incorporated into a framework structure can be attributed to the coordination between the ligand and the metal ions. The narrow emission bands at 563, 598 and 645 nm originate from the Sm(III) lowest emitting state $^4G_{5/2}$ to $^6H_{5/2}$, $^6H_{7/2}$, $^6H_{9/2}$ levels. Considering that the spectra of Sm-MOF not only shows a broad excitation band in the range of 250 - 450 nm, but also exhibits the green (563 nm), orange (598 nm), red (645 nm) emissions of Sm(III) and blue ligand-centered luminescence, it is possible to obtain a single-phase white material by tuning excitation wavelength (Figure S4 and Figure S5). As depicted in Figure 3a, along with the increase of excitation wavelength from 300 to 400 nm, the luminescence intensity of each emission band varies, thus causing that the point of emission spectra in CIE chromaticity diagram (Figure 3b) shifts from red-white (x = 0.3748 and y = 0.2285) to white (x = 0.3093 and y = 0.2316) and the corresponding luminescence color in the photographs (the inset of Figure 3a) changes from red to white. As expected, the white light emission can be realized by the single component Sm(III) framework.

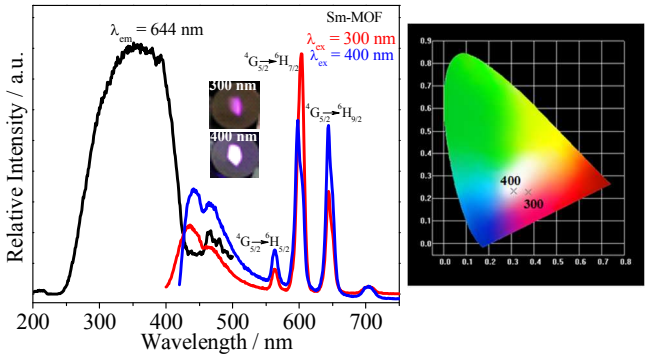

Figure 3 (a) Excitation (black line) and emission spectra (red line λ_{ex} = 300 nm; blue line λ_{ex} = 400 nm) of Sm-MOF (left), and the inset shows its photoluminescence colors with different UV excitation using a Xe lamp as the excitation source. (b) The corresponding CIE chromaticity diagram of Sm-MOF (right) {λ_{ex} = 300 nm (CIE x: 0.3748; CIE y: 0.2285); λ_{ex} = 400 nm (CIE x: 0.3093; CIE y: 0.2316)}.

However, for Dy-MOF, unlike Eu, Tb or Sm-MOF, the emission spectrum of Dy^{3+} is comparatively weaker and shows a much weaker characteristic emission of Dy^{3+} ion at 575 nm corresponding to the $^7F_{9/2} \rightarrow {}^6H_{13/2}$ transition, as shown in Figure S6. The weakness of emission lines in the Dy compound indicates that the selected ligand is not suitable for sensitizing the Dy^{3+} emitters.

From the above luminescent results, the selected ligand NH_2-BDC could effectively sensitize the luminescence of Eu^{3+}, Tb^{3+} and Sm^{3+}, especially the Eu^{3+} ions. And among the four compounds, Eu-MOF possesses longer lifetime and quantum efficiency (Table S1). Therefore, the Eu-MOF was chosen to explore the following sensing behavior for metal ions.

Sensing of mental ions

To examine the potential of the Eu-MOF for the sensing of metal ions, the as-synthesized samples were ground and suspended in DMF solutions containing different metal ions (Li^+, Mn^{2+}, Fe^{2+}, Fe^{3+}, Ni^{2+}, Cu^{2+}, Zn^{2+}, Cd^{2+}, Al^{3+}). The luminescent properties were recorded and compared in Figure 4 and Figure 5. The results revealed that most metal ions have varying degrees of quenching effects on the luminescence intensity. Among the metal ions studied, the quenching effects of Cu^{2+}, Fe^{2+}, Fe^{3+} and Al^{3+} are very pronounced, especially for Al^{3+} ions. The different quenching effects lead to the changes of emitting color under the UV-light irradiation and the luminescence color changes was completely consistent with the variation tendency of the emission spectra in Figure 5. For the Li^+, Mn^{2+}, Zn^{2+}, Cd^{2+} and Ni^{2+} ions, along with quenching effect increasing, the emission intensity at 614 nm is gradually decreasing while the ligand-centered emission in the range of 450 – 550 nm appears, thus leading to the emission color changes from red to pink. For the Cu^{2+}, Fe^{2+}, Fe^{3+} and Al^{3+} ions, although they all seriously quench the emission of Eu^{3+}, their emission colors are different and easy to distinguish under UV light. This is because for Al^{3+} it only completely quenches the emission of Eu^{3+}, while the emission of the

ligand still exists, causing the bright blue light as shown in Figure 4c. However, unlike Al^{3+}, the Cu^{2+}, Fe^{2+} and Fe^{3+} ions can not only quench the emission of Eu^{3+}, but also have quenching effect on the emission of ligand, as a result, their emission colors under UV light are dark.

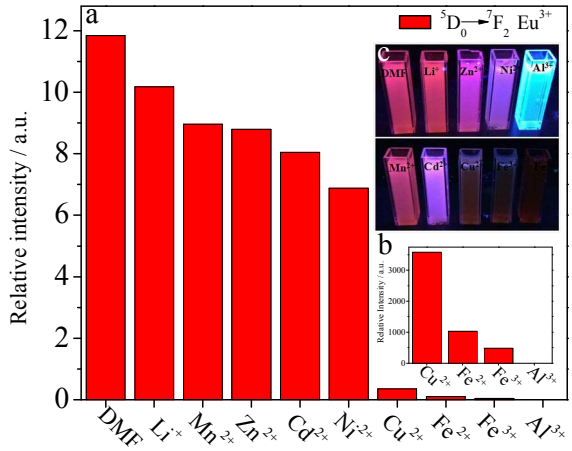

Figure 4 The luminescence intensity of the $^5D_0 \rightarrow {}^7F_2$ transition of Eu-MOF interacting with different metal ions in 10^{-2} mol·L^{-1}DMF solution of MCl_z (excited and monitored at 365 nm). The insets show the relative intensity of Eu-MOF with respect to Cu^{2+}, Fe^{2+}, Fe^{3+} and Al^{3+}(b) and the photographs of M^{z+}·Eu-MOF under UV-light irradiation at 365 nm (c), respectively.

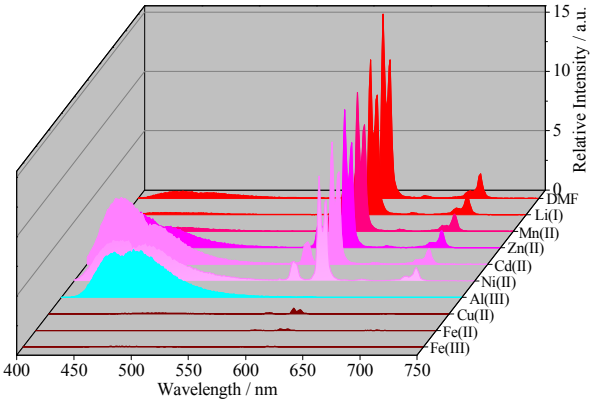

Figure 5 PL spectra of Eu-MOF dispersed into different M^{Z+}-DMF solutions when excited at 365 nm.

To clearly illustrate the different degrees of quenching effects on the ligand emission by the Cu^{2+}, Fe^{2+}, Fe^{3+} and Al^{3+}, the pure ligands were immersed in the DMF solutions containing Cu^{2+}, Fe^{2+}, Fe^{3+} and Al^{3+}, respectively. The luminescent properties of pure ligand in DMF solutions were recorded and compared in Figure 6. As expected, Cu^{2+}, Fe^{2+} and Fe^{3+} totally quench the emission of pure ligands while the Al^{3+} has no significantly quenching effect. Therefore, these results indicate the Eu-MOF can selectively sense Al^{3+} ions through quenching the luminescence of Eu^{3+} rather than that of the ligand. In addition, the luminescence properties of M^{z+} loaded Eu-MOF were further evaluated by fluorescence decay time of Eu^{3+} ion (Figure S8). Most of the metal cations have no significant effects on the luminescence lifetime of Eu^{3+}, while the decay time of Eu-MOF in the presence of Fe^{2+} and Fe^{3+} is undetectable and in the presence of Al^{3+} is 13.96 us, which is basically in agreement with the responses of luminescence of Eu-MOF towards the metal ions.

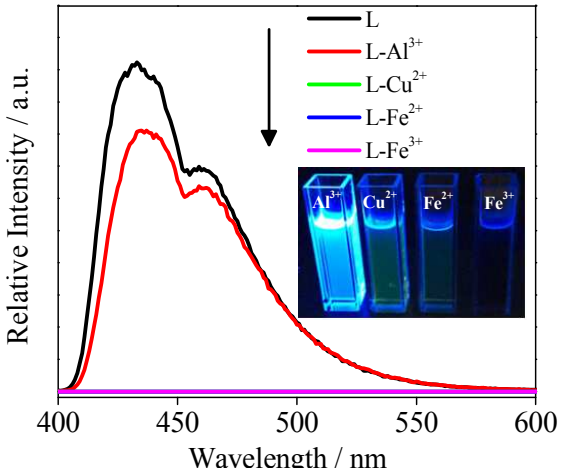

Figure 6 Responses of the fluorescence of pure ligand (NH_2-BDC) towards DMF solution of various metal cations and the inset is the corresponding photograph under UV-light irradiation

Quantitatively, the quenching effect by various metal ions can be rationalized by the Stern -Volmer equation:

$$\frac{I_0}{I} = 1 + K_{sv}[M]$$

I_0 and I are the luminescent intensity before and after metal ion incorporation, respectively. [M] is the metal ion molar concentration. K_{sv} is the quenching coefficient and it was calculated from the experimental data for the examined ions. From the value of K_{sv} in Table 1, it is easy to clearly know that Cu^{2+}, Fe^{2+}, Fe^{3+} and Al^{3+} have strong quenching effect on the luminescence of Eu-MOF.

Table 1 Quenching effect coefficients (K_{sv}) of different metal ions on the luminescence intensity of metal ion-incorporated Eu-MOF.

Metal ions	K_{sv} [M^{-1}]
Li^+	19
Mn^{2+}	33
Zn^{2+}	34
Cd^{2+}	51
Ni^{2+}	75
Cu^{2+}	3146
Fe^{2+}	13224
Fe^{3+}	28786
Al^{3+}	37884

The quenching effect of Eu-MOF was examined as a function of $AlCl_3$ concentration in the range of 0 – 10^{-5} mol·L^{-1}. The Eu-MOF ground samples were immersed in different concentrations of $AlCl_3$, and then concentration-dependent luminescence measurements were also carried out. As shown in Figure 7, for the Al^{3+} loaded sample, the luminescence intensity of Eu^{3+} decreases gradually with the increase of the concentration of Al^{3+}. When the concentration reaches 10^{-4} mol·L^{-1}, the quenching effect on the luminescence of Eu^{3+} is obvious. When the concentration reaches 0.01 mol·L^{-1}, the luminescence is quenched completely and only the emission of the ligand can be seen. Consequently, under the irradiation of UV light of 365 nm, with the increase of Al^{3+}, the colors of the Al^{3+}-loaded samples change from red to blue. At the same time we discovered that the framework of Eu-MOF dissolved gradually and the solution

is completely clear when the concentration of Al^{3+} reached 0.01 mol·L^{-1} (Figure S9). On the basis of these results, we further speculate the possible sensing mechanism.

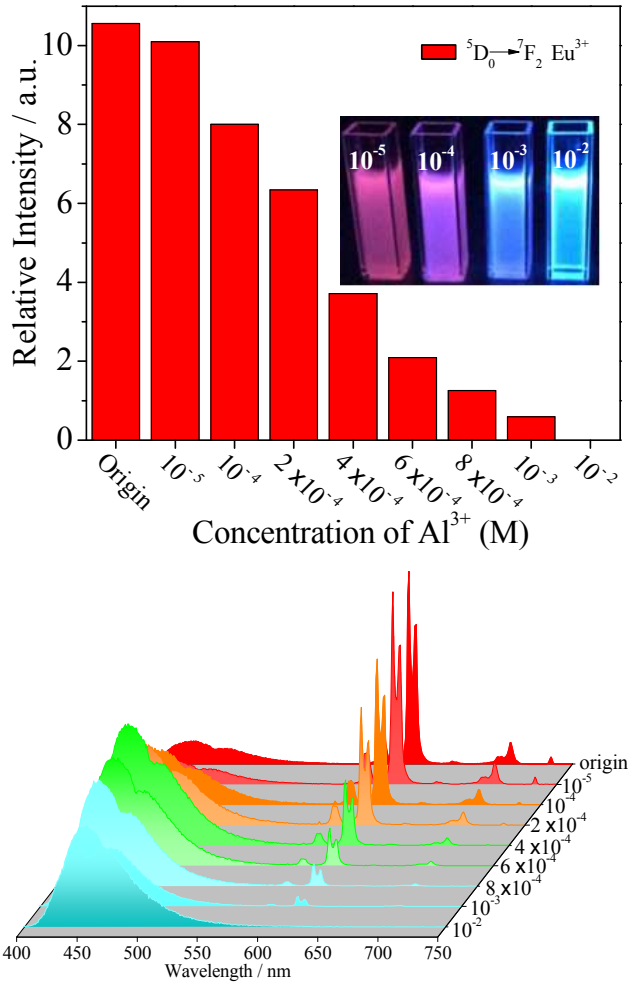

Figure 7 Comparison of the luminescence intensity of Eu-MOF in DMF solutions in the presence of various concentrations of Al^{3+} under excitation at 365 nm.

According to the previous reports, the quenching effect on luminescence MOFs by metal cations may be caused by the following reasons: i) the interaction between metal cations and organic ligands[5d,10,15]; ii) the collapse of the crystal structure[16]; iii) the cation exchange between central cations of MOFs and the targeted cations[17]. In order to elucidate the possible sensing mechanism for the luminescence quenching by the metal ions, the powder XRD (Figure 8) was employed to study on the structural data of the original and M^{z+}-Eu-MOF. For the Li^+, Mn^{2+}, Zn^{2+}, Cd^{2+}, Ni^{2+} and Cu^{2+} ions, their powder XRD are similar to that of Eu-MOF, suggesting that the basic frameworks remain unchanged. Their quenching effects on the luminescence of Eu^{3+} should originate from a less effective transfer process from ligand to the central, which was due to the interaction between metal cations and organic ligands. Whereas, Fe^{2+}/Fe^{3+} and Al3$^+$ loaded Eu-MOF shows a significantly different XRD pattern compared to the original one, implying the crystal structure changed and collapsed. And its quenching effect should be attributed to the complete destruction of the original crystal framework and thus the Eu-based luminescence certainly could not be observed at all (Scheme S1).

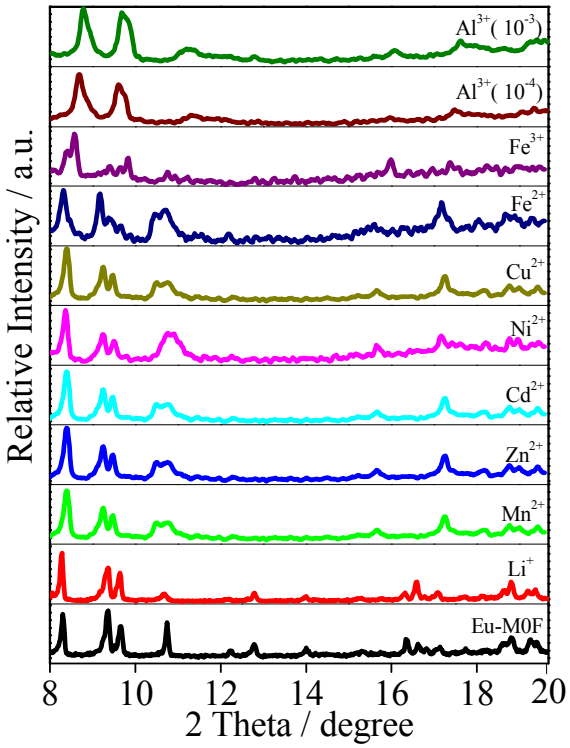

Figure 8 PXRD patterns of the Eu-MOF after immersing in DMF solution with various metal ions.

Conclusions

In summary, four luminescent lanthanide-organic framework (Ln^{3+} = Eu^{3+}, Tb^{3+}, Sm^{3+} and Dy^{3+}), isostructural to MOF-LIC-1(Gd), based on the 2-aminoterephthalic acid are assembled and characterized. Luminescence studies revealed that they all belong to the luminescence materials system with broad excitation band, whose excitation bands all extend to the visible light region. And the fluorescence spectra show the characteristic emission of Ln^{3+}, suggesting that the ligand can effectively sensitize the luminescence of Eu^{3+}, Tb^{3+} and Sm^{3+}, especially the Eu^{3+}. It's worth noting that white light emission could be realized by the single component Sm(III) framework, which provides a promising single component approach to achieve white light emitting materials. Furthermore, Eu-MOF was selected as a representative sample to explore the sensing behavior for metal ions. Most interestingly, compound Eu-MOF performs as a rare example of highly selective and sensitive luminescence sensor for Al^{3+} ions. The emitting color change of this sensor before and after exposure to Al^{3+} is distinguishable even with the naked eyes under the irradiation of UV light of 365 nm. The luminescent mechanism will inspire us to fabricate Ln-MOFs possessing functional sites for specific luminescent selectivity recognition. However, it has been still challenging and more efforts are needed to design Ln-MOFs with proper organic or metal open sites for targeting substrates.

Acknowledgements

This work is supported by the National Natural Science Foundation of China (91122003, 20971100), the Program for New Century Excellent talents in University (NCET-08-0398) and the Developing Science Funds of Tongji University.

Notes and references

Department of Chemistry, Tongji University, Shanghai 200092, China.
Fax: +86-21-65982287; Tel: +86-21-65984663;
E-mail: byan@tongji.edu.cn

Electronic Supplementary Information (ESI) available: [details of any supplementary information available should be included here]. See DOI: 10.1039/b000000x/

1 (*a*) K. Liu, B. Y. Li, Y. Li, X. Li, F. Yang, G. Zing, Y. Peng, Z. J. Zhang, G. H. Li, Z. Shi, S. H. Feng and D. T. Song, *Chem. Commun.*, 2014, **50**, 5031; (*b*) Y. Liu, S. F. Wu, G. Wang, G. P. Yu, J. G. Guan, C. Y. Pan and Z. G. Wang, *J. Mater. Chem. A.*, 2014, **2**, 7795; (*c*) H. M. Yin, J. Q. Wang, Z. Xie, J. H. Yang, J. Bai, J. M. Lu, Y. Zhang, D. H. Yin and J. Y. S. Lin, *Chem. Commun.*, 2014, **50**, 3699; (*d*) H. T. Kwon and H.-K. Jeong, *J. Am. Chem. Soc.*, 2013, **135**, 10763.

2 (*a*) O. Kozachuk, I. Luz, F. X. L. Xamena, H. Noei, M. Kauer, H. B. Albada, E. D. Bloch, B. Marler, Y. M. Wang, M. Muhler and R. A. Fischer, *Angew. Chem. Int. Ed.*, 2014, **53**, 1; (*b*) K. Manna, T. Zhang and W. B. Lin, *J. Am. Chem. Soc.*, 2014, **136**, 6566; (*c*) M. Yoon, R. Srirambalaji and K. Kim, *Chem. Rev.*, 2011, **112**, 1196.

3 (*a*) Z. Q. Xu, W. Meng, H. J. Li, H. W. Hou and Y. T. Fan, *Inorg. Chem.*, 2014, **53**, 3260; (*b*) P. Dechambenoit and J. R. Long, *Chem. Soc. Rev.*, 2011, **40**, 3249.

4 (*a*) Y. N. Wu, M. M. Zhou, S. Li, Z. H. Li, J. Li, B. Z. Wu, G. T. Li, F. T. Li and X. H. Guan, *Small*, 2014; (*b*) S. Rojas, E. Quartapelle-Procopio, F. J. Carmona, M. A. Romero, J. A. R. Navarro and E. Barea, *J. Mater. Chem. B.*, 2014, **2**, 2473.

5 (*a*) D. X. Ma, B. Y. Li, X. J. Zhou, Q. Zhou, K. Liu, G. Zeng, G. H. Li, Z. Shi and S. H. Feng, *Chem. Commun.*, 2013, **49**, 8964; (*b*) M. Zhang, G. Feng, Z. G. Song, Y. P. Zhou, H. Y. Chao, D. Q. Yuan, T. T. Y. Tan, Z. G. Guo, Z. G. Hu, B. Z. Tang, B. Liu and D. Zhao, *J. Am. Chem. Soc.*, 2014, **136**, 7241; (*c*) L. E. Kreno, K. Leong, O. K. Farha, M. Allendorf, R. P. Van Duyne, J. T. Hupp, *Chem. Rev.* 2012, **112**, 1105; (d) Z. M. Hao, X. Z. Song, M. Zhu, X. Meng, S. N. Zhao, S. Q. Su, W. T. Yang, S. Y. Song and H. J. Zhang, *J. Mater. Chem. A.*, 2013, **1**, 11043.

6 (*a*) J. M. Zhou, W. Shi, H. M. Li, H. Li and P. Cheng, *J. Phys. Chem. C.*, 2014, **118**, 416; (*b*) M. Zheng, H. Q. Tan, Z. G. Xie, L. G. Zhang, X. B. Jing and Z. C. Sun, *ACS Appl. Mater. Interfaces.*, 2013, **5**, 1078; (*c*) M. C. Das, G. D. Qian and B. L. Chen, *Chem. Commun.*, 2011, **47**, 11715; (*d*) B. V. Harbuzaru, A. Corma, F. Rey, P. Atienzar, J. L. Jordá, H. García, D. Ananias, L. D. Carlos and J. Rocha, *Angew. Chem. Int. Ed.*, 2008, **47**, 1080; (*e*) B. L. Chen, Y. Yang, F. Zapata, G. N. Lin, G. D. Qian and E. B. Lobkovsky, *Adv. Mater.*, 2007, **19**, 1693.

7 (*a*) S. Liu, Z. Xiang, Z. Hu, X. Zheng and D. Cao, *J. Mater. Chem.*, 2011, **21**, 66493; (*b*) Y. Q. Xiao, Y. J. Cui, Q. Zheng, S. C. Xiang, G. D. Qian and B. L. Chen, *Chem. Comm.*, 2010, **46**, 5503; (*c*) J. L. Bricks, A. Kovalchuk, C. Trieflinger, M. Nofz, M. Büschel, A. I. Tolmachev, J. Daub and K. Rurack, *J. Am. Chem. Soc.*, 2005, **127**, 13522.

8 (*a*) H. B. Zhang, L. J. Zhou, J. Wei, Z. H. Li, P. Lin and S. W. Du, *J. Mater. Chem.*, 2012, **22**, 21210; (*b*) H. H. Li, W. Shi, N. Xu, Z. J. Zhang, Z. Niu, T. Han and P. Cheng, *Cryst. Growth Des.*, 2012, **12**, 2602; (*c*) H. Wang, S. J. Liu, D. Tian, J. M. Jia and T. L. Hu, *Cryst. Growth Des.*, 2012, **12**, 3263; (*d*) P. R. Matthes, C. J. Höller, M. Mai, J. Heck, S. J. Sedlmaier, S. Schmiechen, C. Feldmann, W. Schnick and K. Müller-Buschbaum, *J. Mater. Chem.*, 2012, **22**, 10179; (*e*) B. D. Chandler, D. T. Cramb and G. K. H. Shimizu, *J. Am. Chem. Soc.*, 2006, **128**, 10403.

9 (*a*) J. M. Zhou, W. Shi, N. Xu and P. Cheng, *Inorg. Chem.*, 2013, **52**, 8082;(*b*) B. Zhao, X.Y. Chen, Z. Chen, W. Shi, P. Cheng, S. P. Yan and D. Z. Liao, *Chem. Commun.*, 2009, **21**, 3113; (*c*) H. M. Zhang, H. Yang, L. Z. Wu, S. Song and L. R. Yang, *Bull. Korean Chem. Soc.*, 2012, **33**, 3777; (*d*) J. M. Zhou, H. M. Li, N. Xu and P. Cheng, *Inorg. Chem. Commun.*, 2013, **37**, 30; (*e*) P. J. Calderone, A. M. Plonka, D. Banerjee, Q. A. Nizami and J. B. Parise, *Solid. State. Sci.*, 2013, **15**, 36.

10 B. L. Chen, L. B. Wang, Y. Q. Xiao, F. R. Fronczek, M. Xue, Y. J. Cui and G. D. Qian, *Angew. Chem. Int. Ed.*, 2009, **48**, 500.

11 (*a*) L. L. Wen, L. Zhou, B. G. Zhang, X. G. Meng, H. Qua and D. F. Li, *J. Mater. Chem.*, 2012, **22**, 22603; (*b*) S. Hasegawa, S. Horike, R. Matsuda, S. Furukawa, K. Mochizuki, Y. Kinoshita and S. Kitagawa, *J. Am. Chem. Soc.*, 2007, **129**, 2607; (*c*) Z. Xiang, S. Leng and D. Cao, *J. Phys. Chem. C*, 2012, **116**, 10573; (*d*) Z. Wang, K. K. Tanabe and S. M. Cohen, *Inorg. Chem.*, 2008, **48**, 296.

12 Y. M. Zhu, C. H. Zeng, T. S. Chu, H. M. Wang, Y. Y. Yang, Y. X. Tong, C. Y. Sua and W. T. Wong, *J. Mater. Chem. A.*, 2013, **1**, 11312.

13 J. S. Costa, P. Gamez, C. A. Black, O. Roubeau, S. J. Teat and J. Reedijk, *Eur. J. Inorg. Chem.*, 2008, 1551.

14 L. J. Bellamy, The Infrared Spectra of Complex Molecules; John Wiley& Sons: New York, 1975.

15 Q. Tang, S. X. Liu, Y. W. Liu, J. Miao, S. J. Li, L. Zhang, Z. Shi and Z. P. Zheng, *Inorg. Chem.*, 2013, **52**, 2799.

16 S. Dang, E. Ma, Z. M. Sun and H. J. Zhang, *J. Mater. Chem.*, 2012, **22**, 16920.

17 C. X. Yang, H. B. Ren and X. P. Yan, *Anal. Chem.*, 2013, **85**, 7441.

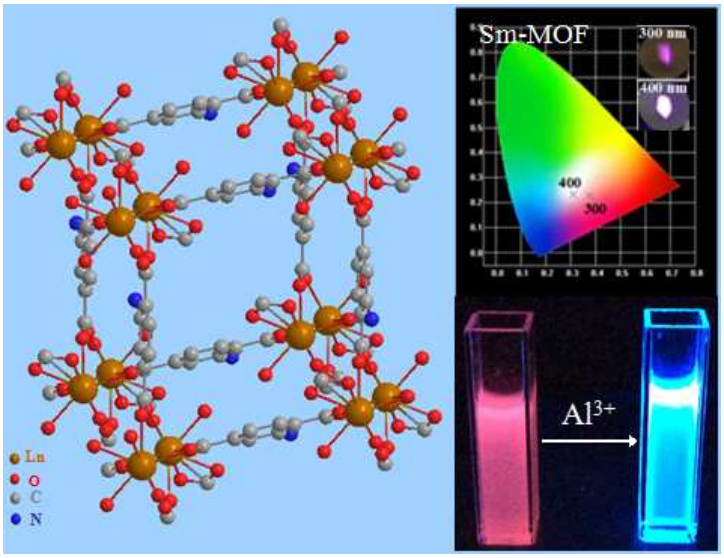

Four luminescent lanthanide-organic framework (Ln = Eu^{3+}, Tb^{3+}, Sm^{3+} and Dy^{3+}), isostructural to MOF-LIC-1(Gd), are assembled. The multi-color are obtained for the system and the white light emission is realized by the single component Sm(III) framework. Most interestingly, Eu-MOF performs highly selective and sensitive luminescence sensor for Al^{3+}.